

# Quantum metrology of noisy spreading channels

Wojciech Górecki,<sup>1</sup> Alberto Riccardi,<sup>2</sup> and Lorenzo Maccone<sup>2</sup>

<sup>1</sup>*Faculty of Physics, University of Warsaw, Pasteura 5, 02-093 Warsaw, Poland*

<sup>2</sup>*Dip. Fisica and INFN Sez. Pavia, University of Pavia, via Bassi 6, I-27100 Pavia, Italy*

We provide the optimal measurement strategy for a class of noisy channels that reduce to the identity channel for a specific value of a parameter (spreading channels). We provide an example that is physically relevant: the estimation of the absolute value of the displacement in the presence of phase randomizing noise. Surprisingly, this noise does not affect the effectiveness of the optimal measurement. We show that, for small displacement, a squeezed vacuum probe field is optimal among strategies with same average energy. A squeezer followed by photodetection is the optimal detection strategy that attains the quantum Fisher information, whereas the customarily used homodyne detection becomes useless in the limit of small displacements, due to the same effect that gives Rayleigh's curse in optical superresolution. There is a quantum advantage: a squeezed or a Fock state with  $N$  average photons allow to asymptotically estimate the parameter with a  $\sqrt{N}$  better precision than classical states with same energy.

The goal of quantum metrology [1, 2] is twofold: (1) estimate the ultimate limits in the estimation of a parameter  $\alpha$  that is encoded into a physical probe by some transformation or channel  $\Lambda_\alpha$ , and (2) find the optimal strategies that attain this limit, namely the ones that achieve the quantum Fisher information on the optimal probe. In the noiseless case, where  $\Lambda_\alpha$  is a unitary transformation, the ultimate limits (the Heisenberg bound) and the optimal estimation strategies are known, and a quantum advantage exists either through entanglement [3] or squeezing [4], typically a quadratic enhancement of  $\sqrt{N}$  in precision, where  $N$  is the number of entangled probes or is the average number of photons (or energy) employed in the estimation. In the noisy case [5, 6], the situation becomes very complicated and noise-dependent: there are many transformations for which all quantum advantage is lost [7] and the optimal detection strategy is known only for a handful of them [2]. In this paper we obtain a local optimal detection strategy for a large class of noisy channels, and we show that a physically relevant one of this class retains the usual  $\sqrt{N}$  quantum advantage. These are channels parametrized by non-negative parameter  $\alpha \geq 0$  that morph into the identity channel for  $\alpha = 0$ . We call them “spreading channels”, since the noise is increased as the parameter increases. More rigorously, a spreading channel  $\Lambda_\alpha$  is defined as having the property  $\lim_{\alpha \rightarrow 0} \Lambda_\alpha[\rho] = \rho$ , with  $\Lambda_\alpha$  differentiable in  $\alpha = 0$ . Our strategies are optimal in the proximity of  $\alpha = 0$ .

The spreading channels may be seen as the ones obtained by the action of a unitary  $U_{\alpha,\varphi} = U_\varphi^\dagger e^{i\alpha G} U_\varphi$  with random, rapidly varying directions  $\varphi$ , distributed according to a distribution  $p(\varphi)$ , which for specific cases was discussed in [8, 9]. A related, but different, problem refers to the “nuisance parameters” [10, 11], where one works under the assumption that the uninteresting (nuisance) parameter  $\varphi$  has values *close* to some *known* value. We drop this assumption here. Note that our analysis is also different from the problem of quantum estimation in the absence of a reference frame [12–14], which can be seen as the action of a rotation  $U_\varphi$  on the final state (we, in contrast, consider a random rotation of the channel itself). For the class of the channels discussed in this paper we show that the averaging over the parameter  $\varphi$  does not affect the efficiency of extracting the information about the parameter  $\alpha$  from the output state.

A physically relevant example of discussed class channels is the estimation of a small value of a displacement  $D(\alpha, \varphi) = e^{\alpha(e^{i\varphi} a^\dagger - e^{-i\varphi} a)}$  of a mode  $a$  of the electromagnetic field in the presence of complete randomization over  $\varphi$  [9, 15]. This is relevant for many estimation procedures, such as for axion dark matter searches [16–19], in communication channels with OOK modulation with dephasing, in magnetic field estimation either at high temperature [8] or in the presence of a trapped ion with unknown phase [9], in gravitational wave detection with resonant cavities, e.g. [20]. Similar issues appear in many optical imaging procedures [21–24].

We show that an optimal probe state among strategies employing the same average energy is the squeezed vacuum. It was previously shown [9, 25] that an optimal probe state is also a highly excited Fock state (which is much more complicated to create, impossible with current technologies). We also show the optimal detection strategy: an anti-squeezing transformation (i.e. a squeezing in the orthogonal direction), followed by a photodetection. Current experiments and proposals use homodyne detection, e.g. [19, 26]. We show that, surprisingly, homodyne detection is not only suboptimal, but even useless in the relevant limit  $\alpha \rightarrow 0$ : a result that corresponds to Rayleigh's curse [21–24], which, after proper formulation, can be seen as a special case of our theorem. A classical state (coherent or thermal) with  $N$  average photons can only attain at most the same sensitivity of the vacuum  $|0\rangle$ , whereas employing a squeezed or a Fock state we find a quantum Fisher information proportional to  $N$  asymptotically for small  $\alpha$ , which proves a  $\sqrt{N}$  enhancement.

We start by providing the precision limits of all spreading channels and showing a simple strategy that attains those limits: a simple yes-no projection onto the initial state of the probe. For the channels coming from averaging of unitary transformations rotated over additional parameter, we show that the Fisher information of the averaged output state is equal to averaged Fisher information calculated for the pure states, so no information is lost. Finally, we study in detail the example of the estimation of a displacement in a channel where the displacement phase is completely randomized.

## I. OPTIMALITY OF SELF-PROJECTION MEASUREMENT

Consider the family of channels depending on the unknown positive parameter  $\alpha \geq 0$  satisfying  $\lim_{\alpha \rightarrow 0} \Lambda_\alpha[\rho] = \rho$  (i.e. they become the identity when  $\alpha = 0$ ).

The aim is to estimate the exact value of  $\alpha$  by using a probe system in the input state  $\rho$  (which may itself be composed of  $N$  entangled sub-probes) and performing the measurement  $\{\Pi_i\}$  on the output state  $\rho_\alpha = \Lambda_\alpha[\rho]$ . This results in a probability distribution  $p(i|\alpha) = \text{Tr}(\Pi_i \rho_\alpha)$ . After  $M$  repetitions we assign the estimator to the sequence of the measurement results  $-\tilde{\alpha}(i_1, i_2, \dots, i_M)$ . From the Cramer-Rao bound (CR), for any unbiased estimator, the RMSE is bounded from below as

$$\Delta\tilde{\alpha} \geq \frac{1}{\sqrt{M} \sqrt{F_C(\rho_\alpha, \{\Pi_i\})}}, \quad (1)$$

where  $F_C(\rho_\alpha, \{\Pi_i\})$  is the classical Fisher information (CFI) (which may depend on number of entangled probes  $N$  used in each repetition). The CR inequality is known to be asymptotically saturable in the limit  $M \rightarrow \infty$ ; in practice the amount of necessary repetitions  $M$  depends on the specific model.

For a given output state  $\rho_\alpha$ , the maximal value of the classical Fisher information is equal to the quantum Fisher information (QFI)

$$\max_{\{\Pi_i\}} F_C(\rho_\alpha, \{\Pi_i\}) = F_Q(\rho_\alpha) := \text{Tr}(\rho_\alpha L^2), \quad (2)$$

where  $L$  is symmetric logarithm derivative  $\frac{d\rho_\alpha}{d\alpha} = \frac{1}{2}(L\rho_\alpha + \rho_\alpha L)$ .

Since the channel is a linear map and the QFI is a convex function, the optimal state for estimating  $\alpha$  is a pure state  $\rho = |\psi\rangle\langle\psi|$ . Below we show, that for any spreading channel, the simple projection measurement on the initial state, i.e.

$$\Pi_0 = |\psi\rangle\langle\psi|, \Pi_1 = \mathbb{1} - \Pi_0 \quad (3)$$

saturates (2) for small values of  $\alpha$ . More precisely, we assume that  $\lim_{\alpha \rightarrow 0^+} F_Q(\rho_\alpha)$  converges to a fixed value  $F_Q^+(\rho_0)$  (see App. A and [27] for a broader technical discussion, which shows that this assumption is inconsequential as long as the value  $\alpha$  is guaranteed to be non-negative). Then we show that

$$F_C(\rho_\alpha, \{\Pi_i\}) = F_Q^+(\rho_0) + \mathcal{O}(\alpha). \quad (4)$$

Proof: the probability of successful projection of the final state  $\rho_\alpha$  onto the initial state, relative to the POVM element  $\Pi_0$  is equal to  $p_0(\alpha) = \text{Tr}(\rho_\alpha |\psi\rangle\langle\psi|)$ . Using the relation between QFI and the fidelity via the Bures metric, for small  $\alpha$  we get

$$\text{Tr}(\rho_\alpha |\psi\rangle\langle\psi|) = 1 - \frac{1}{4} F_Q^+ \alpha^2 + \mathcal{O}(\alpha^3), \quad (5)$$

so

$$p(0|\alpha) = 1 - \frac{1}{4} F_Q^+ \alpha^2 + \mathcal{O}(\alpha^3), \quad p(1|\alpha) = \frac{1}{4} F_Q^+ \alpha^2 + \mathcal{O}(\alpha^3). \quad (6)$$

The CFI for this distribution is

$$F_C(\rho_\alpha, \{\Pi_i\}) = \sum_{i=0,1} \frac{1}{p(i|\alpha)} \left( \frac{\partial}{\partial \alpha} p(i|\alpha) \right)^2 = \frac{1}{p(1|\alpha)[1-p(1|\alpha)]} \left( \frac{\partial}{\partial \alpha} p(1|\alpha) \right)^2 = F_Q^+(\rho_0) + \mathcal{O}(\alpha), \quad (7)$$

which ends the proof.

Two major issues connected with the measurement (3) should be mentioned. Namely, the smaller is  $\alpha$ , the larger is the number of repetitions  $M$  needed to saturate the CR bound, and also the more susceptible to noise is the measurement [28]. For example, consider the noise which changes the probabilities as  $p_0(\alpha) \rightarrow (1-\epsilon)p_0(\alpha) + \epsilon/2$  and  $p_1(\alpha) \rightarrow (1-\epsilon)p_1(\alpha) + \epsilon/2$ . Then, from (7) one can see that in the limit  $\alpha \rightarrow 0$  even arbitrary small  $\epsilon$  may completely decrease the value of Fisher information. In practice, the procedure works well and gives good estimates of  $\alpha$  if the noise  $\epsilon \ll p_1(\alpha)$  and the number of repetitions  $M \gg 1/p_1(\alpha)$ . Note that this issue is not a specific defect of this protocol, but rather an unavoidable difficulty: for certain types of models, maximizing QFI is unavoidably connected with extreme sensitivity to noise [28].

A physically relevant class of spreading channels is the one obtained by averaging some unitary channel over the direction of action. We consider a quantum channel of the form:

$$\Lambda_\alpha(\rho) = \int d\varphi p(\varphi) U_{\alpha,\varphi} \rho U_{\alpha,\varphi}^\dagger, \quad U_{\alpha,\varphi} = U_\varphi^\dagger e^{i\alpha G} U_\varphi. \quad (8)$$

This means that, every time the channel is used,  $\varphi$  is independently randomly drawn from the distribution  $p(\varphi)$ . This is not a randomization of the parameter  $\varphi$  of the probe, but of the channel itself. Assuming a pure input state, from convexity

$$\forall \alpha > 0 \quad F_Q(\rho_\alpha) \leq \int d\varphi p(\varphi) F_Q(|\psi_\alpha^\varphi\rangle) := \overline{F_Q}(\alpha), \quad (9)$$

where  $|\psi_\alpha^\varphi\rangle \equiv U_{\alpha,\varphi} |\psi\rangle$  and  $\overline{F_Q}$  is the average QFI of  $|\psi_\alpha^\varphi\rangle$  over  $\varphi$ . Below we show, that this inequality is tight in the limit of small  $\alpha$  – indeed, for fixed initial state, no information is lost during averaging over  $\varphi$ . Moreover, all this information may be extracted through a projection on the initial state. Indeed, from the Bures metric for pure states we have:

$$|\langle \psi | \psi_\alpha^\varphi \rangle|^2 = 1 - \frac{1}{4} F_Q(|\psi_\alpha^\varphi\rangle) \alpha^2 + \mathcal{O}(\alpha^3), \quad (10)$$

which, after averaging over  $\varphi$ , gives (5) with  $\overline{F_Q}(\alpha)$  in place of  $F_Q^+(\rho_0)$ , which shows that they differ by the factor  $\overline{F_Q}(\alpha) - F_Q^+(\rho_0) = \mathcal{O}(\alpha)$

Note that, if  $p(\varphi)$  is not uniform, some care must be taken to estimate  $\alpha$  from the measurement outcomes, see App. B.

## II. OPTICAL DISPLACEMENT ESTIMATION

In this section we consider a physically relevant example of spreading channels: the estimation of the amplitude  $\alpha$  of a displacement  $D(\alpha, \varphi) = U_\varphi^\dagger e^{i\alpha G} U_\varphi$ , where  $G = \frac{1}{i}(a^\dagger - a)$  and

$U_\varphi = e^{-i\varphi a^\dagger a}$ , with random phase  $\varphi$ . We consider the scenario where the experiment is repeated  $M$  times with a bound  $N$  for the mean input energy in each realization. This is related to typical realistic constrains, where the total number of repetitions  $M$  is restricted by the time of observation, which is independent of the amount of resources used in a single repetition (i.e. one cannot reduce  $N$  increasing  $M$  because of total time constrains). For simplicity of the notation we introduce  $G(\varphi) = U_\varphi^\dagger G U_\varphi = \frac{1}{i}(e^{i\varphi} a^\dagger - e^{-i\varphi} a)$ . For each  $\varphi$ , the QFI is

$$\begin{aligned} F_Q(|\psi_\alpha^\varphi\rangle) &= 4(\langle\psi_\alpha^\varphi|G(\varphi)^2|\psi_\alpha^\varphi\rangle - \langle\psi_\alpha^\varphi|G(\varphi)|\psi_\alpha^\varphi\rangle^2) = \\ &= 4(\langle\psi|G(\varphi)^2|\psi\rangle - \langle\psi|G(\varphi)|\psi\rangle^2) \leq 4\langle G(\varphi)^2\rangle \\ &= 4\langle -e^{2i\varphi} a^{\dagger 2} - e^{-2i\varphi} a^2 + 2a^\dagger a + 1\rangle, \quad (11) \end{aligned}$$

where in the second equality we used the fact that acting with  $e^{iG(\varphi)}$  does not change the variance of  $G(\varphi)$ . Therefore, the average is upper bounded by the average photon number of the initial state as

$$\overline{F_Q} = \frac{1}{2\pi} \int d\varphi F_Q(|\psi_\alpha^\varphi\rangle) \leq 8(\langle a^\dagger a \rangle + \frac{1}{2}) \quad (12)$$

which was derived in a different manner in [9]. This bound can be clearly saturated by a Fock state [9] which is invariant for  $U_\varphi = e^{i\varphi a^\dagger a}$ . What was unknown up to now is that it can also be saturated by a squeezed vacuum state  $|r, 0\rangle$  ( $r$  the squeezing parameter), where for  $\alpha \sim 0$  we have

$$F_Q(|\psi_\alpha^\varphi\rangle) = 8(\cos(2\varphi) \cosh(r) \sinh(r) + \sinh^2(r) + 1/2), \quad (13)$$

where  $N = \langle a^\dagger a \rangle = \sinh^2(r)$ , so indeed after averaging over  $\varphi$ , (12) is saturated. As can be expected, for the squeezing in direction of the shift ( $\varphi \approx 0$ ), the QFI is significantly enhanced, while for the perpendicular direction ( $\varphi \approx \pi/2$ ) it performs even worse than the vacuum state. The intuition behind our procedure is that these competing effects do not cancel (due to the nonlinearity of the QFI) and, after averaging over  $\varphi$ , the bound (12) is saturated. For the optimal measurement proposed in (3) the probability of outcome 0 is exactly given by the fidelity between the initial and final state averaged over  $\varphi$  (the averaging being irrelevant for Fock states). For the squeezed state [29]:

$$\begin{aligned} \int \frac{d\varphi}{2\pi} |\langle r, 0|D(\alpha, \varphi)|r, 0\rangle|^2 &= \\ \int \frac{d\varphi}{2\pi} e^{-\alpha^2(\cos^2(\varphi)e^{2r} + \sin^2(\varphi)e^{-2r})} &= \\ e^{-\alpha^2 \cosh(2r)} I_0(\alpha^2 \sinh(2r)) &= \\ e^{-\alpha^2(2N+1)} I_0(\alpha^2 2\sqrt{N(N+1)}), \quad (14) \end{aligned}$$

with  $I_0$  modified Bessel functions of the first kind, whereas for Fock states [9, 30]:

$$|\langle N|D(\alpha, \varphi)|N\rangle|^2 = e^{-|\alpha|^2 (\mathcal{L}_N(|\alpha|^2))^2}, \quad \forall \varphi \quad (15)$$

with  $\mathcal{L}_N$  the Laguerre polynomial. Both behave in the same way for small  $\alpha$ . So, while both states are equally optimal in

the limit  $\alpha \rightarrow 0$ , for larger values of  $|\alpha|$  the FI for the Fock state is typically higher even though at specific points it is null (see Fig. 1) and there Fock states become useless. So, in the case of local estimation, the Fock state performs better typically, but the situation changes for global estimation since the averaged squeezed state has a monotonic decreasing fidelity, the Fock state does not. So, the value of  $\alpha$  cannot always be derived uniquely solely from the measurement (3) if one uses a Fock state, but it can in the case of squeezed states. Indeed, if one uses a squeezed vacuum, the maximum likelihood estimator  $\tilde{\alpha}_{\text{ML}}(m_0, m_1)$  (where  $m_{0,1}$  are the number of measurements with outcome 0, 1 in the measurement (3)) is simply given by the inverse of the function  $p(0|\alpha)$  (with respect to  $\alpha$ ) at point  $p(0|\alpha) = \frac{m_0}{m_0+m_1}$ . Clearly, when a finite number of measurements are employed, statistical fluctuations in the average (14) will become important, which can be estimated through Monte-Carlo methods (App. C). Up to now, we considered the case where the phase is completely randomized between different measurements. If there is no randomization and the value of  $\varphi$  is known, then the optimal strategy is known [31]: use a squeezed vacuum with  $\varphi$ -dependent squeezing. The intermediate case in which the randomization happens slowly is analyzed in App. D.

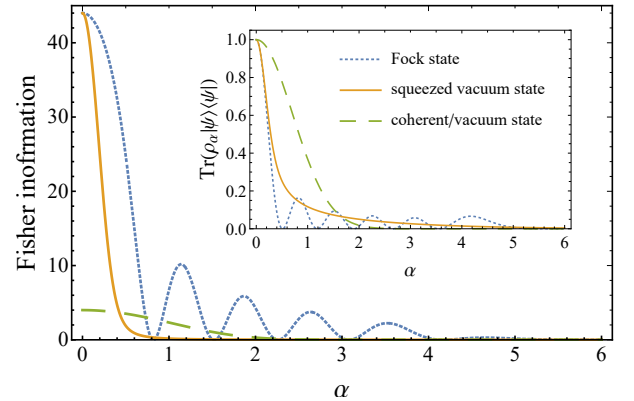


FIG. 1. Classical Fisher information for the measurement (3) and the fidelity (inset) between the initial state  $|\psi\rangle$  and the final state  $|\psi_\alpha^\varphi\rangle = D(\alpha, \varphi)|\psi\rangle$  (with  $D$  displacement), averaged over  $\varphi$  as a function of  $\alpha$ . Blue dotted - Fock state, yellow solid - squeezed vacuum state, green dashed - coherent state, all with  $N = 5$  average photons. For the vacuum state the fidelity is the same as for coherent state (green dashed).

The quantum enhancement can be shown if one starts from a coherent state  $|\beta\rangle$  with average number of photons  $|\beta|^2$ , it is clear that

$$|\langle \beta|D(\alpha, \varphi)|\beta\rangle|^2 = |\langle 0|D(\alpha, \varphi)|0\rangle|^2 = e^{-\alpha^2}, \quad (16)$$

namely, the fidelity between a coherent state and a displaced coherent state is the same as the fidelity between the vacuum and the displaced vacuum for the same degree of displacement. So one can obtain a strategy that performs equally well using a zero-energy vacuum state instead of a coherent state (and both are impervious to the value of  $\varphi$  which does not affect the fidelity). In the context of (12), the inequality is not

saturated in this case, since for general coherent state  $|\beta\rangle$  the term  $\langle\beta|G(\varphi)|\beta\rangle$  (appearing in (11)) has non zero value.

Thermal states will perform worse. So, it is clear that any classical strategy of energy  $|\beta|^2 = N$  is, at best, as effective as a strategy that uses a vacuum state (which is the optimal strategy for zero energy). In contrast, (12) shows that the optimal quantum strategy of energy  $N$  has QFI of order  $N$ . While this resembles the typical  $\sqrt{N}$  enhancement in precision of quantum strategies vs. classical ones in quantum metrology, interestingly it has a different origin than usual: it originates from the fact that any energy devoted to classical strategies is completely useless, rather than from a different allocation of the resources.

Both Fock state and squeezed states may help with the problem with noise susceptibility discussed after (7). Indeed, looking at (14) one can see that for large  $N$  the probability of getting result 0 is approximately a function of  $\sim \alpha^2 N$ , so even for extremely small values of the parameter one is able to keep the probability of the result 1 sufficiently large, by increasing the energy.

We now comment on the practicalities of the two strategies. On one hand, the Fock state strategy [9, 30] requires that the initial state of the radiation be prepared in  $|N\rangle$ . There is no currently known technique to prepare such state for the electromagnetic field which is scalable to high values of  $N$ . Then, at the detection stage one must project onto the initial state  $|N\rangle$ , which can be implemented with a photon-number resolving photodetector. Such devices exist, but cannot retain effective photon-number resolution to large numbers  $N$  of photons. On the other hand, the squeezed state strategy seems more practical, since there is a vast literature for the preparation of squeezed states at different wavelengths spanning from the optical [32] to the microwave [33]. At the detection stage, one must evaluate the probability that the output state of the channel  $|\psi_\alpha^\varphi\rangle$  is equal to a squeezed vacuum, namely  $p(0|\alpha) = |\langle 0|S^\dagger(r)|\psi_\alpha^\varphi\rangle|^2$ , where  $|r, 0\rangle = S(r)|0\rangle$ . This expression can be also interpreted as the calculation of the overlap between the state  $S^\dagger|\psi_\alpha^\varphi\rangle$  with the vacuum state  $|0\rangle$ , which can be easily implemented: the first is the state obtained by applying the inverse squeezing transformation  $S^\dagger$  after the channel and then performing a photodetection. The probability to obtain zero photons at the measurement will give  $p(0|\alpha)$ , whereas the probability to obtain one or more photons will give  $p(1|\alpha)$ . An avalanche photodiode (APD) or any equivalent avalanche photodetector (e.g. transition edge sensors) will provide such output signal in the ideal case. The whole procedure must be gated so that it is clear when a “no

click” must be interpreted as an outcome.

It might seem surprising that one must un-squeeze the signal before the detection, since the state preparation involves a squeezing transformation: however, the squeezing, channel application and un-squeezing is equivalent to a (sub-shot noise) effective amplification of the quadrature, whenever the signal is orthogonal to the squeezing. In general, this condition is not warranted but, as shown in the previous section, this is irrelevant: after the averaging over  $\varphi$ , this procedure still performs very well, and it performs optimally for small values of  $\alpha$ , which is the regime of interest.

One could think that an alternative detection for the squeezed strategy could be implemented through homodyne detection, by measuring the quadrature of the light consistent with the squeezing phase. While this strategy may be useful in some cases, surprisingly in the regime of small  $\alpha$ , this strategy fails in a way reminiscent of Rayleigh’s curse [21, 24] for the evaluation of the distance of two point sources (while the last problem also may easily be described within our formalism by taking  $|\psi\rangle \propto \exp(-x^2/4\sigma^2)|x\rangle$ ,  $G = \frac{1}{i}\partial_x$ ,  $p(\varphi) = \frac{1}{2}(\delta(\varphi) + \delta(\varphi - \pi))$ ; see App. E for broader discussion about relation between these two models).

### III. CONCLUSIONS

We have provided the optimal estimation strategy for the spreading parameter  $\alpha$  of spreading noisy channels, where some other parameter  $\varphi$  is randomized. This is one of the very few instances where we can give the optimal metrology strategy for a noisy channel. We analyzed a specific instance of spreading channels: the estimation of the amplitude of a displacement with random phase. We show a quantum enhancement equal to the square root of the number of photons employed in the estimation and we derived a new optimal strategy, based on squeezed vacuum states, that is practically implementable with current techniques, in contrast to the previously known one [9, 25] based on Fock states.

This material is based upon work supported by the U.S. Department of Energy, Office of Science, National Quantum Information Science Research Centers, Superconducting Quantum Materials and Systems Center (SQMS) under contract number DE-AC02-07CH11359. W. G. acknowledges support from the National Science Center (Poland) Grant No. 2020/37/B/ST2/02134 and the Foundation for Polish Science (FNP) via the START scholarship. We acknowledge useful feedback from M. Sacchi and R. Demkowicz-Dobrzański.

---

[1] V. Giovannetti, S. Lloyd, L. Maccone, *Advances in Quantum Metrology*, *Nature Phot.* **5**, 222 (2011).  
 [2] R. Demkowicz-Dobrzański, M. Jarzyna, J. Kolodyński, *Quantum Limits in Optical Interferometry*, *Progress in Optics* **60**, 345 (2015).  
 [3] V. Giovannetti, S. Lloyd, L. Maccone, *Quantum metrology*, *Phys. Rev. Lett.* **96**, 010401 (2006).  
 [4] L. Maccone, A. Ricciardi, *Squeezing Metrology: a unified*

*framework*, *Quantum* **4**, 292 (2020).  
 [5] R. Demkowicz-Dobrzański, J. Kolodyński, and M. Guta, *Nature Comm.* **3**, 1063 (2012).  
 [6] B.M. Escher, R.L. de Matos Filho, and L. Davidovich, *Nature Phys.* **7**, 406 (2011).  
 [7] J. Kolodyński, R. Demkowicz-Dobrzański, *Phase estimation without a priori phase knowledge in the presence of loss*, *Phys. Rev. A* **82**, 053804 (2010).

- [8] R. Nichols, T. R. Bromley, L. A. Correa, and G. Adesso, Practical quantum metrology in noisy environments, *Phys. Rev. A* **94**, 042101 (2016).
- [9] F. Wolf, C. Shi, J. C. Heip, M. Gessner, L. Pezzé, A. Smerzi, M. Schulte, K. Hammerer, P. O. Schmidt, Motional Fock states for quantum-enhanced amplitude and phase measurements with trapped ions, *Nature Comm.* **10**, 2929 (2019).
- [10] J. Suzuki, Y. Yang, M. Hayashi, Quantum state estimation with nuisance parameters, *J. Phys. A: Math. Theor.* **53**, 453001 (2020).
- [11] J. Suzuki, Nuisance parameter problem in quantum estimation theory: tradeoff relation and qubit examples, *J. Phys. A: Math. Theor.* **53**, 264001 (2020).
- [12] K. Banaszek, A. Dragan, W. Wasilewski, and C. Radzewicz, Experimental demonstration of entanglement-enhanced classical communication over a quantum channel with correlated noise, *Phys. Rev. Lett.* **92**, 257901 (2004).
- [13] S. D. Bartlett, T. Rudolph, and R. W. Spekkens, Reference frames, superselection rules, and quantum information, *Rev. Mod. Phys.* **79**, 555 (2007).
- [14] M. Fanizza, M. Rosati, M. Skotiniotis, J. Calsamiglia, and V. Giovannetti, Squeezing-enhanced communication without a phase reference, *Quantum* **5**, 608 (2021).
- [15] R. Yousefjani, R. Nichols, S. Salimi, G. Adesso, Estimating phase with a random generator: Strategies and resources in multiparameter quantum metrology, *Phys. Rev. A* **95**, 062307 (2017).
- [16] K. Backes, D. Palken, S. Kenany, B. Brubaker, S. Cahn, A. Droster, G. Hilton, S. Ghosh, H. Jackson, S. Lamoreaux, A quantum enhanced search for dark matter axions, *Nature* **590**, 238 (2021).
- [17] J. Teufel, T. Donner, M. Castellanos-Beltran, J. Harlow, K. Lehnert, Nanomechanical motion measured with an imprecision below that at the standard quantum limit, *Nature Nanotech.* **4**, 820 (2009).
- [18] R. Dassonneville, R. Assouly, T. Peronin, A. Clerk, A. Bienfait, B. Huard, Dissipative Stabilization of Squeezing Beyond 3 dB in a Microwave Mode, *PRX Quantum* **2**, 020323 (2021).
- [19] A. J. Brady, C. Gao, R. Harnik, Z. Liu, Z. Zhang, Q. Zhuang, Entangled sensor-networks for dark-matter searches, *arXiv:2203.05375* (2022).
- [20] R. Ballantini, P. Bernard, E. Chiaveri, A. Chincarini, G. Gemme, R. Losito, R. Parodi, E. Picasso, A detector of high frequency gravitational waves based on coupled microwave cavities, *Class. Quantum Grav* **20**, 3505 (2003).
- [21] M. Tsang, R. Nair, and X.-M. Lu, Quantum Theory of Super-resolution for Two Incoherent Optical Point Sources, *Phys. Rev. X* **6**, 031033 (2016).
- [22] M. Tsang, Subdiffraction incoherent optical imaging via spatial-mode demultiplexing, *New J. Phys.* **19**, 023054 (2017).
- [23] M. Tsang, Quantum limit to subdiffraction incoherent optical imaging, *Phys. Rev. A* **99**, 012305 (2019).
- [24] W.-K. Tham, H. Ferretti, A. M. Steinberg, Beating Rayleigh's Curse by Imaging Using Phase Information, *Phys. Rev. Lett.* **118**, 070801 (2017).
- [25] F. Hanamura, W. Asavanant, K. Fukui, S. Konno, A. Furusawa, Estimation of Gaussian random displacement using non-Gaussian states, *Phys. Rev. A* **104**, 062601 (2021).
- [26] K. M. Backes et al., A quantum enhanced search for dark matter axions, *Nature* **590**, 238 (2021).
- [27] S. Zhou, L. Jiang, An exact correspondence between the quantum Fisher information and the Bures metric, *arXiv:1910.08473v1* (2019).
- [28] S. Kurdzialek and R. Demkowicz-Dobrzanski, Measurement noise susceptibility in quantum estimation, *arXiv:2206.12430* (2022).
- [29] J. Brask, Gaussian states and operations, a quick reference, *arXiv:2102.05748* (2021).
- [30] F. Oliveira, M. Kim, P. Knight, V. Buek, Properties of displaced number states, *Phys. Rev. A* **41**, 2645 (1990).
- [31] H.P. Yuen, Two-photon coherent states of the radiation field *Phys. Rev. A* **13**, 2226 (1976).
- [32] V.V. Dodonov, 'Nonclassical' states in quantum optics: a 'squeezed' review of the first 75 years, *J. Opt. B: Quantum Semiclass. Opt.* **4**, R1 (2002).
- [33] R. Dassonneville, R. Assouly, T. Peronin, A.A. Clerk, A. Bienfait, B. Huard, Dissipative Stabilization of Squeezing Beyond 3 dB in a Microwave Mode, *PRX Quantum* **2**, 020323 (2021).
- [34] W.H. Zurek, Sub-Planck structure in phase space and its relevance for quantum decoherence, *Nature* **412**, 712 (2001).
- [35] G. M. D'Ariano, C. Macchiavello, and L. Maccone, Quantum tomography of mesoscopic superpositions of radiation states, *Phys. Rev. A* **59**, 1816 (1999).
- [36] A. Ourjoumtsev, R. Tualle-Brouri, J. Laurat, P. Grangier, Generating Optical Schrödinger Kittens for Quantum Information Processing, *Science* **312**, 83 (2006).
- [37] B. Vlastakis, G. Kirchmair, Z. Leghtas, S.E. Nigg, L. Frunzio, S. M. Girvin, M. Mirrahimi, M. H. Devoret, R. J. Schoelkopf, Deterministically Encoding Quantum Information Using 100-Photon Schrödinger Cat States, *Science* **342**, 607 (2013).
- [38] M.G.A. Paris, Quantum estimation for quantum technology, *Int. J. Quantum Inf.* **7**, 125 (2009).

#### Appendix A: Discontinuity of QFI at $\alpha = 0$

In this appendix we recall a simple example from [27] to show that the issues mentioned in [27] do not affect our reasoning in the case we are interested in. Namely, the situation when the parameter  $\alpha$  to be estimated is non-negative.

Consider the family of states:

$$\rho_\alpha = \alpha^2 |0\rangle\langle 0| + (1 - \alpha^2) |1\rangle\langle 1| \quad (\text{A1})$$

and let  $\alpha$  be an arbitrary real number. Then for any point different from  $\alpha = 0$ , the symmetric logarithmic derivative is equal to

$$L = \frac{2}{\alpha} |0\rangle\langle 0| - \frac{2\alpha}{1-\alpha^2} |1\rangle\langle 1|, \quad (\text{A2})$$

which leads to a QFI

$$F_Q(\rho_\alpha) = \text{Tr}(\rho_\alpha L^2) = 4 + \frac{4\alpha^2}{1-\alpha^2}, \quad (\text{A3})$$

so  $\lim_{\alpha \rightarrow 0^+} F_Q(\rho_\alpha) = 4$ . However, for  $\alpha = 0$ , the symmetric logarithmic derivative is simply  $L = 0$ , so also  $F_Q(\rho_\alpha)|_{\alpha=0} = 0$ . The simple interpretation of this fact is that the state  $\rho_\alpha$  does not distinguish between positive and negative values of  $\alpha$ , so any measurement performed on it cannot allow for local estimation of  $\alpha$  around point  $\alpha = 0$  (while for any different point  $\alpha \neq 0$  local estimation will be possible). It is clear that, in our case, where we consider only non-negative  $\alpha$ , this issue does not appear, so it is reasonable to consider  $F_Q^+(\rho_0)$  instead of  $F_Q(\rho_\alpha)|_{\alpha=0} = 0$ .

## Appendix B: Estimator of $\alpha$

In order to recover the value of  $\alpha$ , one must know the actual form of the probability distribution  $p(\varphi)$ , since the maximum likelihood estimator is obtained from the theoretical probability of obtaining the results which, in turn, depends on  $p(\varphi)$ . Indeed, the maximum likelihood estimator is

$$\tilde{\alpha}_{ML}(k_0, k_1) := \arg \max_{\alpha} p(k_0, k_1 | \alpha), \quad (\text{B1})$$

where  $k_{0/1}$  the number of results 0/1. Therefore, if one has no a priori knowledge on  $p(\varphi)$  we cannot simply assume that the distribution is uniform, as it may lead to a strongly biased estimator. However, one can add an additional random-uniform rotation, so that the overall rotation becomes uniformly distributed. Indeed, assume that  $\varphi$  is non-uniform distributed with some unknown function  $p(\varphi)$ . Add an additional rotation of the initial state  $U_{\theta} |\psi\rangle$  as well as a final rotation prior to the measurement  $U_{\theta} \Pi_0 U_{\theta}^{\dagger}$ . Then,

$$p(0|\alpha) = \int p(\varphi) d\varphi \int_0^{2\pi} \frac{d\theta}{2\pi} |\langle \psi | \psi_{\alpha}^{\theta+\varphi} \rangle|^2 = \int_0^{2\pi} \frac{d\theta}{2\pi} |\langle \psi | \psi_{\alpha}^{\theta} \rangle|^2, \quad (\text{B2})$$

which leads to the same statistics as an initial uniform distribution of  $\varphi$ . Of course, this is in general a suboptimal strategy, as the mean value of the QFI for uniform distribution may be smaller than the one for the true  $p(\varphi)$ . In practice, it will usually be better to spend some resources to find an estimate to  $p(\varphi)$  and then use the rest to estimate  $\alpha$ .

## Appendix C: Performance of different types of initial states

In this section we analyze the performance of other initial states, in addition to the squeezed vacuum and Fock states considered in the main text. Moreover, we present some Monte-Carlo simulations that show how the squeezed vacuum (and the other states) perform when considering a finite number  $M$  of repetitions of the experiment with randomly varying phase  $\varphi$  (in the main text we considered the simple case in which the randomization is perfect).

Consider the multi-cat state [34]

$$|\text{cat}_{N,\theta}\rangle \propto \sum_{n=1}^N |\exp(2i\pi n/N + i\theta)\beta\rangle, \quad (\text{C1})$$

namely a superposition of  $N$  coherent states with equispaced phases. As shown in Fig. 2, this is a good approximation for the Fock state already for moderate values of  $N$ , and it may be simpler to create in practice: at least for  $N = 2$  it can be created in quantum optics, e.g. [35, 36] or in the microwave regime also for  $N = 3, 4$  [37].

In Fig. 3 we consider various states: the coherent state  $|\beta\rangle$ , the vacuum state  $|0\rangle$ , the squeezed state  $|r, \theta\rangle$ , the multicat  $|\text{cat}_{N,\theta}\rangle$  for different values of  $N$  and  $\theta$ . We plot the overlap

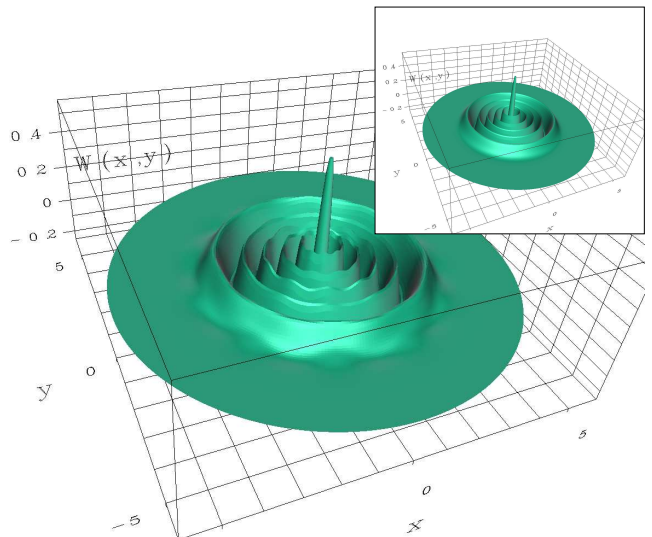


FIG. 2. Wigner function of the multi-cat  $|\text{cat}_{N,\theta}\rangle$  with  $N = 10$  and 10 average photons, i.e.  $\beta \simeq 8.3045$  in Eq. (C1). It is evident that such a state closely approximates a Fock state with the same number of photons (inset).

between each of these states and its displaced version after a displacement  $D(\alpha, \varphi)$  with a fixed phase. A good metrological state is the one that is highly sensitive to  $\alpha$ , namely whose value changes rapidly as a function of  $\alpha$ . In Fig. 4 we present a Monte-Carlo simulation that shows how the randomly varying  $\varphi$  affects the overlap. As expected (see also Fig. 1), the random phase ruins the metrological sensitivity of the more phase-sensitive states. Yet, in the regime of small  $\alpha$  we are interested in, the squeezed state  $|r, 0\rangle$  and the two-cat state  $|\text{cat}_{N=2,\theta}\rangle$  still behave as well as the Fock state which is insensitive to  $\varphi$ .

## Appendix D: Slowly varying $\varphi$

Up to now we have assumed that the rotation  $\varphi$  changes randomly from one shot to the next. In practice, there might be a slow time dependence such that the value of  $\varphi$  is reasonably constant for some time: consider a time-dependent probability  $p(\varphi|t)$ , which gives  $p(\varphi)$  of (8) when averaged over a large time interval, but which is sufficiently tight for a short period of time. Then one can use a feedback strategy in which one quickly performs an estimate of  $\varphi$  and then uses it to prepare a squeezed vacuum with squeezing parameter orthogonal to  $\varphi$ . Such a state performs better than the Fock state, as long as the value of  $\varphi$  is known. Alternatively, instead of first estimating  $\varphi$  and then using its value in the subsequent measurements, one could also employ multiparameter estimation [38].

In essence, the bounds to precision presented in this paper can be beaten under the hypothesis that the random parameter  $\varphi$  changes sufficiently slowly.

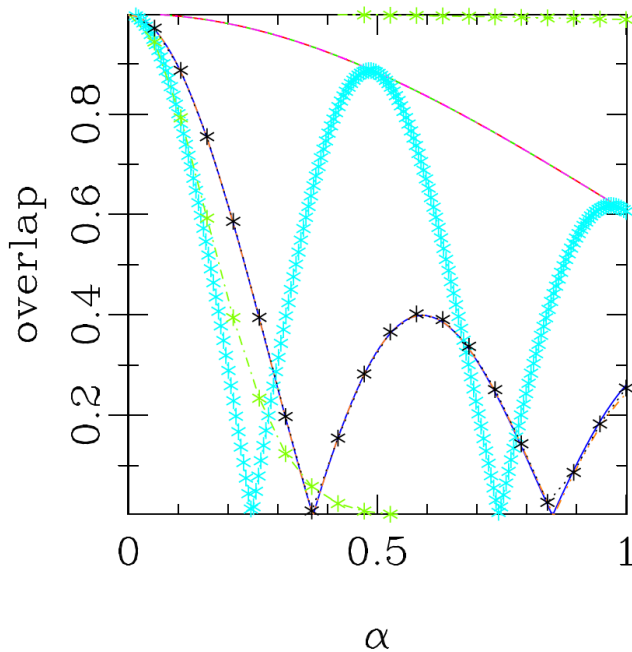


FIG. 3. Plot of the overlap between the initial state and the initial state displaced by  $D(\alpha, \varphi)$  (here with fixed phase  $\varphi$ ) as a function of  $\alpha$ . Namely,  $overlap = |\langle \psi | \mathcal{D}(\alpha) | \psi \rangle|$  where  $|\psi\rangle$  is any of the states we consider here. The squeezed vacuum state  $|r, \theta\rangle$  (green stars with dash-dotted line) performs worse if the squeezing phase  $\theta$  is parallel to the displacement phase  $\varphi$  (upper curve) and it performs very well if the two phases are orthogonal (lower curve). The coherent state, the vacuum state and the two-cat state with phase  $\theta$  parallel to the displacement all perform equally (higher solid multi-colored curve). They all perform quite badly: the overlap decreases very little as a function of  $\alpha$ . The multi-cat state  $|\text{cat}_{N,\theta}\rangle$  (here we use  $N = 10$  cats) is plotted as the continuous blue curve for parallel phase  $\theta$  and as the orange dot-dashed curve for orthogonal phase  $\theta$  (they are indistinguishable in this plot as there is little difference between their performance: the multi-cat is almost insensitive to phase). In contrast, the two-cat state is quite sensitive to the phase  $\theta$ : the cyan dotted curve plots its performance when its phase is orthogonal to the displacement (good behavior), whereas it behaves exactly as the coherent state if the phase is parallel. The best state overall appears to be the 2-cat state (but is highly phase-sensitive). In contrast, the Fock state (black line) is basically identical to the multi-cat and are both independent on the phase (the Fock is exactly independent, the multi-cat is approximately independent). All states here (except for the vacuum state) have the same average number of photons,  $\langle a^\dagger a \rangle = 10$ .

#### Appendix E: Quadrature measurement and Rayleigh's curse

In this section we analyze how a quadrature measurement compares to the projection onto the initial state that was considered in the main text. Surprisingly, we show that, even though this measurement strategy performs well for large values of  $\alpha$ , it does not work well in the regime of asymptotically small  $\alpha$  we are interested in.

This failure mode is somewhat reminiscent of the Rayleigh's curse in discriminating two point-like sources at

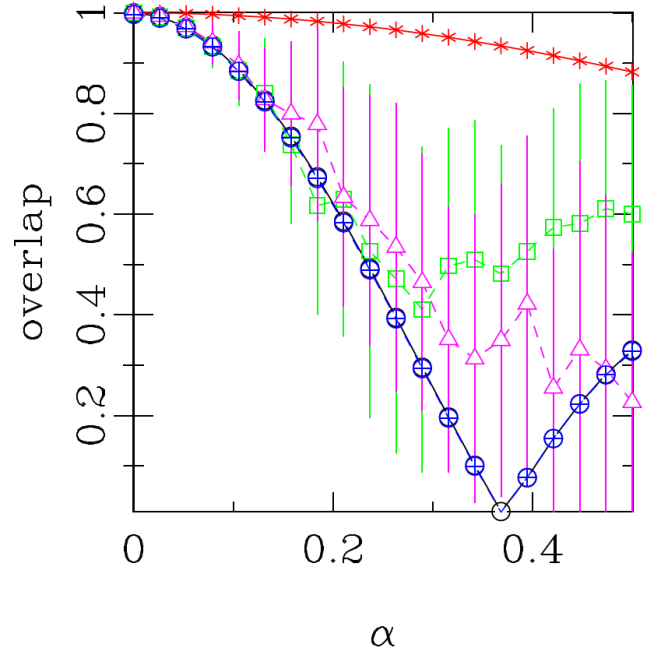


FIG. 4. Monte-Carlo simulation of the overlap between the initial state and the initial state displaced by  $D(\alpha, \varphi)$  with randomly chosen  $\varphi$  as a function of  $\alpha$ . The coherent state/vacuum (red stars), the Fock state (black lines) and the 10-cat (blue circles) are unaffected (the multi-cat is affected slightly, but the effects cannot be seen at this scale). The two-cat (green squares) is quite phase sensitive and the fluctuations for random phases can be easily seen (vertical bars). The squeezed vacuum (pink triangles) is also very sensitive to phase. In the regime  $\alpha \rightarrow 0$ , the Fock state, the squeezed vacuum, the two-cat and the 10-cat all perform in a similar way. The vertical bars are not the statistical error bars: they are an estimation of the fluctuations (the root mean square of the overlap). [The error bars would be the root mean square divided by the square root of the number of simulated phases.] Here all states (except the vacuum) have  $\langle a^\dagger a \rangle = 10$  and an average over  $M = 50$  uniformly distributed random values of  $\varphi$  is performed.

a distance using a finite-aperture lens. It is known that using a quantum optimized detection strategy, the Rayleigh's curse can be beaten [21]. Analogously, in the estimation of  $\alpha$  in the regime  $\alpha \rightarrow 0$ , the quadrature measurement fails, whereas the projection onto the initial state is optimal.

Consider estimating the value of  $\alpha$  from measuring the quadrature of the light in a direction consistent with the initial squeezing. I.e. for an initial squeezed state with zero phase, consider the measurement of the zero-phase quadrature, namely

$$\hat{x} = \frac{1}{\sqrt{2}}(a + a^\dagger) \quad (\text{E1})$$

Since  $\varphi$  is uniformly distributed, the expected value of the quadrature is  $\langle \hat{x} \rangle = 0$ , so  $\alpha$  cannot be simply estimated from its mean value. Can we use the second moment or the variance  $\langle \hat{x}^2 \rangle$ ? Consider the observable  $A = \hat{x}^2$ . On the squeezed

vacuum, displaced and averaged over  $\varphi$ , we find

$$\langle A \rangle = \alpha^2 + \frac{1}{2}e^{-2r}, \quad \langle \Delta^2 A \rangle = e^{-2r} (2\alpha^2 + \frac{1}{2}e^{-2r}), \quad (\text{E2})$$

Error propagation gives:

$$\Delta^2 \tilde{\alpha} = \frac{\langle \Delta^2 A \rangle}{|\partial_\alpha \langle A \rangle|^2} = \frac{e^{-2r}(4\alpha^2 + e^{-2r})}{8\alpha^2}. \quad (\text{E3})$$

For  $\alpha^2 \gg e^{-2r}$  we find  $\Delta^2 \tilde{\alpha} \approx \frac{1}{2}e^{-2r}$ . It means that the variance scales as the inverse of the mean energy of the input state, which is the optimal scaling, as shown in (12). However, for  $\alpha^2 \ll e^{-2r}$ , the variance scales inversely to  $\alpha^2$  and goes to infinity for  $\alpha \rightarrow 0$ . This is closely related to the Rayleigh curse [21]. In fact, in our problem the output state may be written in following form:

$$\begin{aligned} \rho_\alpha &= \int_0^{2\pi} \frac{d\varphi}{2\pi} |\psi_\alpha^\varphi\rangle \langle \psi_\alpha^\varphi| = \\ &= \int_0^\pi \frac{d\varphi}{\pi} \frac{1}{2} (|\psi_\alpha^\varphi\rangle \langle \psi_\alpha^\varphi| + |\psi_\alpha^{\varphi+\pi}\rangle \langle \psi_\alpha^{\varphi+\pi}|) = \\ &= \int_0^\pi \frac{d\varphi}{\pi} \frac{1}{2} (|\psi_\alpha^\varphi\rangle \langle \psi_\alpha^\varphi| + |\psi_{-\alpha}^\varphi\rangle \langle \psi_{-\alpha}^\varphi|). \quad (\text{E4}) \end{aligned}$$

The convexity of classical Fisher information implies

$$\begin{aligned} F_C(\rho_\alpha, \Pi_x) &\leq \\ &= \int_0^\pi \frac{d\varphi}{\pi} F_C \left( \frac{1}{2} (|\psi_\alpha^\varphi\rangle \langle \psi_\alpha^\varphi| + |\psi_{-\alpha}^\varphi\rangle \langle \psi_{-\alpha}^\varphi|), \Pi_x \right). \quad (\text{E5}) \end{aligned}$$

Moreover, for any  $\varphi$ ,

$$\lim_{\alpha \rightarrow 0} F_C \left( \frac{1}{2} (|\psi_\alpha^\varphi\rangle \langle \psi_\alpha^\varphi| + |\psi_{-\alpha}^\varphi\rangle \langle \psi_{-\alpha}^\varphi|), \Pi_x \right) = 0. \quad (\text{E6})$$

The last equation may be proved for any reasonable initial state (the precise criteria will be given later), not only for squeezed vacuum state. Indeed, for the state  $\frac{1}{2} (|\psi_\alpha^\varphi\rangle \langle \psi_\alpha^\varphi| + |\psi_{-\alpha}^\varphi\rangle \langle \psi_{-\alpha}^\varphi|)$  the probability of getting the result  $x$  has the form

$$\begin{aligned} p(x|\alpha) &= \text{Tr}(\Pi_x \frac{1}{2} (|\psi_\alpha^\varphi\rangle \langle \psi_\alpha^\varphi| + |\psi_{-\alpha}^\varphi\rangle \langle \psi_{-\alpha}^\varphi|)) = \\ &= \frac{1}{2} (f(x + \sqrt{2}\alpha \cos(\varphi)) + f(x - \sqrt{2}\alpha \cos(\varphi))), \quad (\text{E7}) \end{aligned}$$

where  $f(x) = \text{Tr}(\Pi_x |\psi\rangle \langle \psi|)$ . This implies

$$\lim_{\alpha \rightarrow 0} \frac{\partial p(x|\alpha)}{\partial \alpha} = 0 \quad \forall x. \quad (\text{E8})$$

Since  $F_C$  is given by:

$$F_C = \int dx \frac{1}{p(x|\alpha)} \left( \frac{\partial p(x|\alpha)}{\partial \alpha} \right)^2, \quad (\text{E9})$$

then equation (E8) does not immediately lead to the conclusion that the CFI vanishes, since we need to pay special attention to the points where also  $\lim_{\alpha \rightarrow 0} p(x|\alpha) = 0$  (since in principle it may lead to non-zero Fisher information, as in the example discussed in App. A).

Let us restrict to the functions  $f(x)$  which have a continuous second derivative with respect to  $x$ . Moreover, let us assume that there exists an integrable function  $g(x)$  such that  $\forall_{x,\alpha} \frac{1}{p(x|\alpha)} \left( \frac{\partial p(x|\alpha)}{\partial \alpha} \right)^2 \leq g(x)$  (which is satisfied for both the squeezed vacuum state and the Fock state discussed in this paper). Then, from the dominated convergence theorem

$$\lim_{\alpha \rightarrow 0} F_C = \int dx \lim_{\alpha \rightarrow 0} \frac{1}{p(x|\alpha)} \left( \frac{\partial p(x|\alpha)}{\partial \alpha} \right)^2. \quad (\text{E10})$$

For any point where  $f(x) \neq 0$ , obviously  $\frac{1}{p(x|\alpha)} \left( \frac{\partial p(x|\alpha)}{\partial \alpha} \right)^2 = 0$ . Where  $f(x) = 0$ :

$$\begin{aligned} p(x|\alpha) &= \cos^2(\varphi) \alpha^2 \partial_x^2 f(x) + \mathcal{O}(\alpha^3) \\ \partial_\alpha p(x|\alpha) &= 2 \cos^2(\varphi) \alpha \partial_x^2 f(x) + \mathcal{O}(\alpha^2) \end{aligned} \quad (\text{E11})$$

and therefore:

$$\lim_{\alpha \rightarrow 0} \frac{1}{p(x|\alpha)} \left( \frac{\partial p(x|\alpha)}{\partial \alpha} \right)^2 = \begin{cases} 0 & \text{if } f(x) = 0 \\ 4 \cos^2(\varphi) \partial_x^2 f(x) & \text{if } f(x) \neq 0 \end{cases} \quad (\text{E12})$$

Note, that for any function  $f(x)$ , which have a continuous second derivative, there could be at least countably many points where simultaneously  $f(x) = 0$  and  $\partial_x^2 f(x) \neq 0$ , so the value of the integral (E10) is equal to 0 anyway.

In conclusion, in the limit  $\alpha \rightarrow 0$ , the measurement (3) is much more informative than measuring quadrature, which is, in general a poor measurement in this regime.